

Solid-State ^{95}Mo NMR Studies of Some Prototypal Molybdenum Compounds: Sodium Molybdate Dihydrate, Hexacarbonylmolybdenum, and Pentacarbonyl Phosphine Molybdenum(0) Complexes

Klaus Eichele,[†] Roderick E. Wasylshen,^{*,†} and John H. Nelson[‡]

Departments of Chemistry, Dalhousie University, Halifax, Nova Scotia, Canada B3H 4J3, and University of Nevada, Reno, Nevada 89557-0020

Received: April 10, 1997[⊗]

Molybdenum-95 nuclear quadrupolar coupling constants, $\chi(^{95}\text{Mo})$, and quadrupolar asymmetry parameters, η , for sodium molybdate dihydrate, hexacarbonylmolybdenum(0), pentacarbonyl-5-methyldibenzophospholemolybdenum(0), and pentacarbonylbis(diphenylphosphino)methanemolybdenum(0) were obtained from solid-state ^{95}Mo NMR measurements at 26 MHz (9.4 T). The first direct measurements of $^1J(^{95}\text{Mo},^{13}\text{C})$ and $^1J(^{95}\text{Mo},^{31}\text{P})$ from solid-state ^{95}Mo NMR spectra are reported. Also, the first example of a $^{13}\text{C}/^{12}\text{C}$ isotope effect on ^{95}Mo shielding is reported for solid $\text{Mo}(\text{CO})_6$: $^1\Delta\text{Mo}(^{13}/^{12}\text{C}) = -0.316$ ppm. Direct-dipolar spin–spin interactions involving protons and molybdenum (*i.e.*, $^1\text{H}-^{95}\text{Mo}$) are relatively weak and do not appear to make significant contributions to ^{95}Mo NMR line shapes when spectra are acquired with magic-angle spinning. Hexacarbonylmolybdenum is proposed as a useful setup sample for solid-state ^{95}Mo NMR studies. Our results for the pentacarbonyl phosphine molybdenum complexes indicate that solid-state ^{95}Mo NMR studies should be feasible for a range of molybdenum(0) octahedral complexes. These studies will be facilitated by using applied magnetic fields well above 10 T.

Introduction

Molybdenum has two naturally abundant NMR-active isotopes, ^{95}Mo ($I = 5/2$, NA = 15.72%) and ^{97}Mo ($I = 5/2$, NA = 9.46%).^{1,2} The magnitudes of their respective nuclear magnetic moments are small; both are slightly smaller than that of ^{14}N . The nuclear quadrupole moment, eQ , for ^{95}Mo is relatively small compared to that of most other quadrupolar nuclei in the NMR periodic table and more than an order of magnitude smaller than that of ^{97}Mo : $eQ(^{97}\text{Mo})/eQ(^{95}\text{Mo}) = -11.47$. The nuclear properties of ^{95}Mo are sufficiently favorable that ^{95}Mo NMR chemical shifts for hundreds of compounds have been reported.^{1–5} Almost every study has been a solution ^{95}Mo NMR study; *i.e.*, it involved the investigation of molybdenum compounds dissolved in isotropic solvents. Under conditions of extreme narrowing, ^{95}Mo NMR peaks in solution samples are expected to be sharper than corresponding ^{97}Mo NMR peaks by a factor of approximately 132. A very recent comprehensive review of the ^{95}Mo NMR literature by Malito² cited more than 150 original papers. Approximately one-third of a page of the review ($\ll 1\%$) was devoted to ^{95}Mo NMR studies of solids; only four studies were specifically mentioned. The author incorrectly states that there were no solid-state ^{95}Mo NMR studies prior to 1985 (*vide infra*); however, it is certainly true that very few have been reported. Solid-state NMR studies have been hampered by the relatively low NMR receptivity of $^{95/97}\text{Mo}$, long probe dead-times, and acoustic ringing associated with the pulse-NMR observation of low-frequency NMR nuclides, particularly those with rapidly decaying time-domain spectra. Given the scarcity of solid-state $^{95/97}\text{Mo}$ NMR data available in the literature, we felt that it would be worthwhile to characterize a few simple compounds which might serve as benchmarks for future researchers. Specifically,

the purpose of this paper is to present some new experimental molybdenum chemical shift and quadrupolar coupling data. Accurate ^{95}Mo NMR data for a few readily available compounds should assist future researchers interested in applying solid-state ^{95}Mo NMR as a research tool. Reliable $^{95/97}\text{Mo}$ nuclear quadrupolar coupling constants are available for very few compounds. Also, this study reports the first direct measurements of $^1J(^{95}\text{Mo},^{13}\text{C})$ and $^1J(^{95}\text{Mo},^{31}\text{P})$ in the solid state and the first report of a $^{12}\text{C}/^{13}\text{C}$ isotope effect on molybdenum shielding.

Theory

The Hamiltonian governing the ^{95}Mo single-quantum NMR spectrum is composed of the Zeeman interaction, the chemical shielding (CS) and the nuclear quadrupolar interactions.^{6–9} For a stationary sample, the frequency of a given transition, $m \leftrightarrow m - 1$, can be described by

$$\nu = \nu_0 - \nu^\sigma + \nu^{(1)}_{m,m-1} + \nu^{(2)}_{m,m-1} \quad (1)$$

where ν_0 is the Larmor frequency,

$$\nu_0 = \frac{\gamma B_0}{2\pi} \quad (2)$$

and the anisotropic chemical shielding is given by:

$$\nu^\sigma = \nu_0(\sigma_{11} \sin^2 \theta \cos^2 \phi + \sigma_{22} \sin^2 \theta \sin^2 \phi + \sigma_{33} \cos^2 \theta) \quad (3)$$

where the principal components of the chemical shielding tensor are defined relative to the bare nucleus with $\sigma_{33} \geq \sigma_{22} \geq \sigma_{11}$. The polar angles ϕ and θ describe the orientation of the external magnetic field, \mathbf{B}_0 , in the principal axis system (PAS) of the chemical shielding tensor. In practice, NMR spectroscopists generally measure chemical shifts, the differences in shielding constants between the nuclei of interest and a nucleus of the

* Address correspondence to this author. Phone: 902-494-2564. Fax: 902-494-1310. E-mail: Roderick.Wasylshen@Dal.Ca.

[†] Dalhousie University.

[‡] University of Nevada.

[⊗] Abstract published in *Advance ACS Abstracts*, July 1, 1997.

reference sample. The components of the chemical shift tensor will be defined using the convention: $\delta_{11} \geq \delta_{22} \geq \delta_{33}$ (note that δ_{33} corresponds to the most shielded direction of the chemical shift tensor).

The nuclear quadrupole coupling is an electrostatic interaction between the nuclear quadrupole moment, eQ , and the symmetric electric-field gradient (EFG) tensor, $e\mathbf{q}$, at the nucleus.¹⁰ In its PAS, the principal components of \mathbf{q} are defined in a right-handed fashion such that $|q_{33}| \geq |q_{22}| \geq |q_{11}|$. Because the quadrupolar interaction is traceless, two parameters are sufficient to define the magnitude of the principal components, the quadrupolar coupling constant χ and the asymmetry parameter η :

$$\chi = e^2 Q q_{33} / h \quad (4)$$

$$\eta = (q_{11} - q_{22}) / q_{33} \quad (5)$$

In order to describe the ⁹⁵Mo NMR spectra of the compounds investigated in this study, both first- and second-order quadrupolar terms will be considered⁷⁻⁹

$$\nu_{m,m-1}^{(1)} = (\nu_Q/4)(1 - 2m)[3 \cos^2 \vartheta - 1 + \eta \cos 2\varphi \sin^2 \vartheta] \quad (6)$$

$$\nu_{m,m-1}^{(2)} = (\nu_Q^2/12\nu_0)\{^{3/2} \sin^2 \vartheta [(A + B) \cos^2 \vartheta - B] - \eta \cos 2\varphi \sin^2 \vartheta [(A + B) \cos^2 \vartheta + B] + (\eta^2/6)[A - (A + 4B) \cos^2 \vartheta - (A + B) \cos^2 2\varphi (\cos^2 \vartheta - 1)^2]\} \quad (7)$$

with

$$\nu_Q = \frac{3\chi}{2I(2I - 1)} \quad (8)$$

$$A = 24m(m - 1) - 4I(I + 1) + 9 \quad (9)$$

$$B = \frac{1}{4}[6m(m - 1) - 2I(I + 1) + 3] \quad (10)$$

where the polar angles φ and ϑ describe the orientation of the external magnetic field in the PAS of the EFG tensor.

The frequencies of the four satellite transitions (⁵/₂ ↔ ³/₂, ³/₂ ↔ ¹/₂, ⁻¹/₂ ↔ ⁻³/₂, ⁻³/₂ ↔ ⁻⁵/₂) are determined by the chemical shielding and first- and second-order quadrupolar interactions, while the frequency of the central transition (¹/₂ ↔ ⁻¹/₂) depends only on chemical shielding and second-order quadrupolar interactions.

Under conditions of rapid sample spinning about the magic angle, the NMR line shape of the central transition depends only on the magnitude of the quadrupolar coupling constant and the asymmetry parameter. If the satellite transitions are excited by the rf-pulse, the powder line shape will break up into a series of spinning sidebands. The intensity profile of the sidebands depends upon the same parameters that describe the spectrum of a stationary sample: the EFG tensor, the CS tensor, and their relative orientation. Expressions which enable one to calculate the spectra of spinning samples can be found elsewhere.^{6,8,9}

Finally, in the presence of a spin-1/2 nucleus, S , coupled to the quadrupolar nucleus, the magic-angle spinning (MAS) line shape of the central transition will exhibit an additional splitting due to the indirect spin-spin coupling interaction

$$\nu(m_S) = \nu - m_S J_{iso} \quad (11)$$

where ν describes eq 1 under MAS, J_{iso} is the isotropic indirect

spin-spin coupling constant, and m_S is the z component of the S nuclear spin in the external field ($m_S = \pm 1/2$).

Experimental Section

Sodium molybdate dihydrate and hexacarbonylmolybdenum(0) were commercially available. Pentacarbonyl-5-methyldibenzophosphole molybdenum(0), Mo(CO)₅(MeDBP), was prepared as previously described,¹¹ and pentacarbonylbis(diphenylphosphino)methanemolybdenum(0), Mo(CO)₅(η¹-dppm), was prepared using standard literature methods.¹²

All ⁹⁵Mo NMR spectra were acquired at 26 MHz using a Bruker AMX-400 (9.4 T) spectrometer. Molybdenum chemical shifts were referenced with respect to an external aqueous alkaline 2 M solution of Na₂MoO₄ (pH ≈ 11).¹³ All chemical shifts were corrected for the second-order quadrupolar interaction. Solid-state ⁹⁵Mo NMR spectra were acquired using a Bruker double-bearing MAS probe with 7 mm zirconia rotors. Although ¹H decoupling at 400 MHz was not possible using this probe, ¹H-⁹⁵Mo direct-dipolar coupling interactions in the samples investigated in this study are sufficiently weak that they can be eliminated by spinning the sample at the magic angle. The 90° pulse length, 7.0–8.1 μs, was determined for the solution reference sample. Except for the ⁹⁵Mo spectra of Mo(CO)₆, solid-state spectra were acquired after a single “selective” 90° pulse, which is one-third of the “solution” 90° pulse. The spectra often displayed a rolling base line due to acoustic ringing and were corrected using a cubic spline base line correction.

Solid-state ⁹⁵Mo NMR spectra were simulated using CSolids, a program developed in this laboratory. For calculating spectra of static samples, anisotropic shielding and first- and second-order quadrupolar interactions were taken into account. Transition probabilities were taken from the literature.⁶ For spectra of the central transition obtained with rapid MAS, only the quadrupolar interaction to second order was considered, together with potential indirect spin-spin coupling. Calculation of spectra under slow spinning conditions was performed in the time domain with anisotropic shielding and first-order quadrupolar interactions considered.

Results and Discussion

Molybdenum-95 NMR parameters obtained in this study are summarized in Table 1.

Sodium Molybdate Dihydrate, Na₂MoO₄·2H₂O. The ⁹⁵Mo NMR spectrum of solid Na₂MoO₄·2H₂O obtained with magic-angle spinning is shown in Figure 1. This is a typical MAS NMR spectrum arising from the central transition (¹/₂ ↔ ⁻¹/₂) of a noninteger quadrupolar nucleus. The observed ⁹⁵Mo NMR line shape depends only on the ⁹⁵Mo nuclear quadrupolar coupling constant, $\chi(^{95}\text{Mo})$, and the asymmetry parameter, η . The ⁹⁵Mo nuclear quadrupolar coupling constant of 1.15 MHz determined for solid Na₂MoO₄·2H₂O indicates significant departure from tetrahedral symmetry at the molybdenum nucleus. Furthermore, the large asymmetry in the EFG tensor, $\eta = 0.85$, indicates the absence of C₃ symmetry at the molybdenum nucleus. These conclusions are in agreement with the reported crystal structure which indicates that alternate layers of MoO₄²⁻ distorted tetrahedra and water molecules are connected by interlinking sodium cations and hydrogen bonds.¹⁴ In any given molybdate ion, the four Mo–O bond lengths are different (1.768, 1.788, 1.752, and 1.781 Å) and the six O–Mo–O bond angles also differ and fall in the range 107.6°–112.7°. The crystal is orthorhombic, space group *Pbca* with $Z = 8$. The eight molybdate ions are crystallographically

TABLE 1: Solid-State ^{95}Mo NMR Data for Some Model Compounds

compound	δ_{iso}^a (ppm)	χ (MHz)	η	reference
$\text{Na}_2\text{MoO}_4 \cdot 2\text{H}_2\text{O}$	8 4	1.15	0.82	this study ^b Edwards <i>et al.</i> ^c
$\text{Mo}(\text{CO})_6$	-1854 ^d -1854 -1854 -1852 -1857	0.091 0.141	0.142 <0.1	this study ^b Nolle ^e Edwards <i>et al.</i> ^c Shirley ^f Mastikhin <i>et al.</i> ^g
$\text{Mo}(\text{CO})_5(\text{MeDBP})$	-1825 ^h -1812	(-1.03) ⁱ	0.25	this study ^b Maitra <i>et al.</i> ^j
$\text{Mo}(\text{CO})_5(\eta^1\text{-dppm})$	-1775 ^k -1764	1.31	0.3	this study ^b Alyea <i>et al.</i> ^l
$\text{Mo}(\text{CO})_5(\text{PPh}_3)$		1.972	0.064	Blumer <i>et al.</i> ^m
<i>cis</i> - $\text{Mo}(\text{CO})_4(\text{PPh}_3)_2$		2.919	0.07 \pm 0.07	Blumer <i>et al.</i> ^m

^a ^{95}Mo chemical shifts are reported with respect to an external 2 M aqueous solution of Na_2MoO_4 at a pH of approximately 11. ^b Chemical shifts are corrected for the second-order quadrupolar shift. ^c Reference 15. ^d $\delta_{11} = -1843$ ppm, $\delta_{22} = -1855$ ppm, $\delta_{33} = -1865$ ppm, $\alpha = 90^\circ$, $\beta = 90^\circ$, $\gamma = 50^\circ$, $^1J(^{95}\text{Mo}, ^{13}\text{C}) = 69$ Hz. ^e Reference 18. ^f Physisorbed on calcined alumina, chemical shift is given with respect to 1 M Na_2MoO_4 at pH = 9; the line width at 9.4 T is reported as 230 Hz; reference 19. ^g Reference 17. ^h $^1J(^{95}\text{Mo}, ^{31}\text{P}) = 122$ Hz. ⁱ The sign was deduced from residual $^{95}\text{Mo}, ^{31}\text{P}$ dipolar splittings in ^{31}P CP/MAS spectra. ^j Measured in CH_2Cl_2 solution, $^1J(^{95}\text{Mo}, ^{31}\text{P}) = 129$ Hz; reference 11. ^k $^1J(^{95}\text{Mo}, ^{31}\text{P}) = 130$ Hz. ^l Measured in CH_2Cl_2 solution, $^1J(^{95}\text{Mo}, ^{31}\text{P}) = 140$ Hz; reference 39. ^m Data were obtained from NQR transitions at 77 K; reference 36.

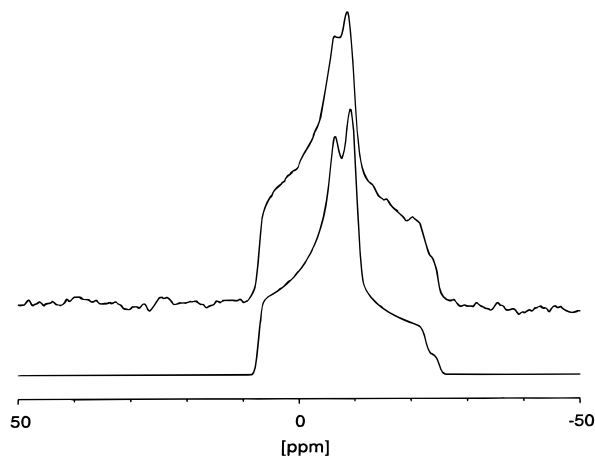


Figure 1. ^{95}Mo MAS NMR spectra of a solid powder sample of $\text{Na}_2\text{MoO}_4 \cdot 2\text{H}_2\text{O}$ obtained at 9.4 T. The experimental spectrum is shown on the top trace; 22 070 scans, 4 s recycle delay, spinning rate 2.35 kHz. The theoretical spectrum shown on the lower trace was calculated using the values given in Table 1.

equivalent, thus the ^{95}Mo NMR spectrum of a powder sample is identical for all eight molybdate ions.

Sample spinning at 2.35 kHz was sufficient to effectively eliminate all spinning sidebands except for weak first-order spinning sidebands. Examination of a ^{95}Mo NMR spectrum obtained for a stationary sample indicates that the chemical shift tensor has a span of approximately 200 ppm; however, the quality of our spectra does not permit further analysis. It is interesting that ^{95}Mo NMR spectra of $\text{Na}_2\text{MoO}_4 \cdot 2\text{H}_2\text{O}$ were previously investigated by Edwards *et al.*¹⁵ at the same applied magnetic field (9.4 T) as used in the present study. The ^{95}Mo MAS NMR line shape was featureless, presumably because of the 200 Hz line broadening applied before Fourier transformation of the free-induction decay. In simulating the spectrum shown in Figure 1, the calculated spectrum was convoluted with a Gaussian peak of only 30 Hz. Clearly, the ^1H - ^{95}Mo direct-dipolar interactions are sufficiently weak that they are effectively eliminated by MAS at moderate spinning frequencies.

In contrast to the dihydrate, the anhydrous salt of sodium molybdate, Na_2MoO_4 , is apparently cubic.¹⁶ This compound was the subject of an early continuous wave solid-state ^{23}Na and ^{95}Mo NMR investigation by Lynch and Segel¹⁶ who found no evidence of a quadrupole interaction for ^{95}Mo . This conclusion has been confirmed by the more recent pulse-Fourier transform measurements of Mastikhin *et al.*¹⁷ The latter authors found $\delta(\text{Mo}) = -35 \pm 5$ ppm with respect to an external 1 M aqueous solution of Na_2MoO_4 .

Hexacarbonylmolybdenum, $\text{Mo}(\text{CO})_6$. The ^{95}Mo NMR spectrum of solid hexacarbonylmolybdenum was first reported by Nolle in 1977.¹⁸ The spectrum of a powder sample was examined at 2.11 and 2.24 T. Spectra of stationary samples and samples spinning at 60 Hz perpendicular to the applied magnetic field were obtained and analyzed. Only the central transition, $1/2 \leftrightarrow -1/2$, was observed. The spectrum of a stationary sample at 2.11 T exhibited a small splitting (74.7 ± 4.3 Hz) with a line shape characteristic of that expected when only the second-order quadrupolar interaction is important. On this basis, Nolle¹⁸ reported $\nu_Q = 21.1 \pm 2.3$ kHz where $\nu_Q = 3\chi/2(2I - 1)$; thus for $I = 5/2$, $\nu_Q = 3\chi/20$ and Nolle's result corresponds to $\chi = 141 \pm 15$ kHz. The asymmetry parameter was found to be less than 0.1. Other researchers^{15,17,19} have examined the ^{95}Mo NMR spectrum of solid $\text{Mo}(\text{CO})_6$ but appear to be unaware of the work of Nolle.¹⁸ While Edwards *et al.*¹⁵ recognized that it was possible to observe features in their spectra from transitions other than the central transition, they apparently did not attempt to analyze the spectra. It appears that Mastikhin *et al.*¹⁷ did not observe any of the satellite transitions, and from the relatively narrow peak arising from the central transition they concluded that the EFG tensor at the Mo nucleus was 0. No evidence for anisotropic shielding of the molybdenum nucleus of $\text{Mo}(\text{CO})_6$ has been reported previously.

We have obtained ^{95}Mo NMR spectra of stationary and spinning samples of polycrystalline $\text{Mo}(\text{CO})_6$. In addition to characterizing the EFG tensor, we have been able to determine the principal components of the molybdenum chemical shift tensor and establish the relative orientation of the EFG and shift tensors. Spectra are shown in Figures 2 and 3, and the results of our analysis are summarized in Table 1.

The ^{95}Mo NMR spectrum of a stationary sample of $\text{Mo}(\text{CO})_6$ is shown in Figure 2, together with the best-fit calculated spectrum. In this case, the line shape of the central transition, $1/2 \leftrightarrow -1/2$, is completely dominated by anisotropic chemical shielding; the second-order quadrupolar splitting is calculated to be less than 10 Hz, *ca.* 0.4 ppm (for systems where $\eta \approx 0$, the second-order quadrupolar splitting can loosely be defined as the splitting between the maxima in the "Pake-like" doublet). The principal components of the chemical shift (CS) tensor are $\delta_{11} = -1843 \pm 1$ ppm, $\delta_{22} = -1855 \pm 1$ ppm, and $\delta_{33} = -1865 \pm 1$ ppm. As already mentioned, the prominent features of the powder pattern arising from the satellite transitions depend on the magnitude of the quadrupolar coupling constant, the asymmetry of the EFG tensor, the principal components of the CS tensor, and the relative orientation of the EFG and CS tensors. In analyzing the spectrum in Figure 2, the components of the chemical shift tensor were obtained from the central transition and the quadrupolar parameters of Nolle¹⁸ were used as starting parameters in fitting the satellite transitions. The results of our analysis indicate that $\chi(^{95}\text{Mo}) = 91$ kHz, $\eta = 0.142$, the direction of greatest shielding, δ_{33} , lies along q_{22} , and both δ_{11} and δ_{22} lie in the $q_{11} - q_{33}$ plane as shown in Figure 2. One might ask why the magnitude of $\chi(^{95}\text{Mo})$ obtained here is much less than the value reported by Nolle (*i.e.*, 91 kHz *vs*

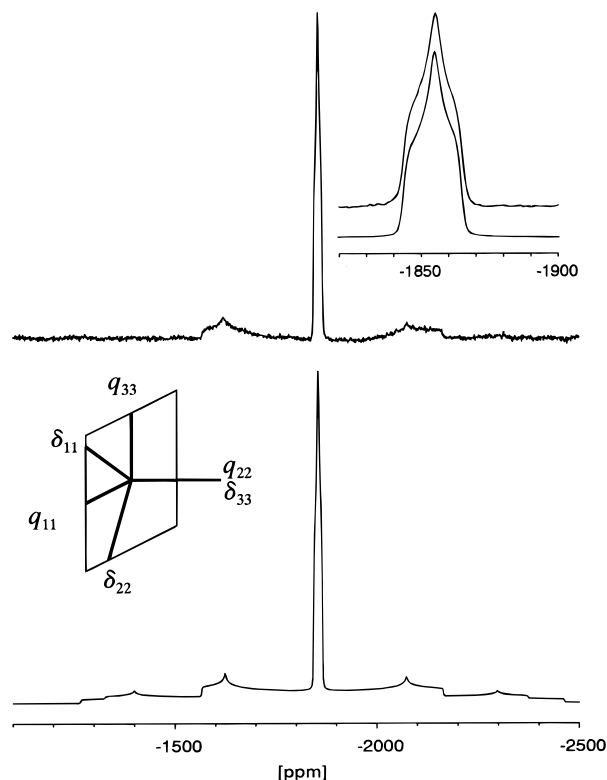


Figure 2. ^{95}Mo NMR spectra of a static powder sample of $\text{Mo}(\text{CO})_6$ obtained at 9.4 T. The experimental spectrum is shown on the top trace; 7624 scans, 10 s recycle delay, 10 Hz line broadening. The theoretical spectrum shown on the lower trace was calculated using the values given in Table 1 and convoluted with a Gaussian peak of 70 Hz width. Weak outermost shoulders due to the satellite transitions fall outside the frequency range shown (see Figure 3). The upper inset shows an expansion of the central transition illustrating the importance of the anisotropic chemical shielding interaction. The lower inset indicates the relative orientation of the molybdenum chemical shift and electric field gradient tensors.

141 kHz). Anisotropic chemical shielding was not considered in the early low-field NMR study of Nolle;¹⁸ however, from our results at 9.4 T, it is clear that the span of the shift tensor at 2.11 T is approximately 130 Hz. At 2.11 T, the second-order quadrupolar splitting for a stationary sample is approximately 32 Hz. That is, the line shape at 2.11 T will be influenced by both interactions but anisotropic shielding is the dominant interaction in determining the line shape of the central transition for a static sample. Using the parameters obtained in our study, we can reproduce the experimental spectra shown in ref 18.

In order to further confirm that the second-order quadrupolar splitting is negligible at 9.4 T, ^{95}Mo NMR spectra were obtained with MAS (see Figure 3). The half-height line width of the central transition is about 6 Hz, whereby approximately 3 Hz are accounted for by the second-order quadrupolar splitting. Observed and calculated spectra are compared in Figure 3. Given that the rf-pulse power is insufficient to uniformly excite the total span of the spectrum, agreement between the observed and calculated spectrum is excellent. One feature in the MAS spectrum deserving of comment is the weak peaks which flank the central transition (see inset, Figure 3). These weak peaks arise from ^{95}Mo – ^{13}C indirect spin–spin coupling, $^1J(^{95}\text{Mo},^{13}\text{C}) = 69 \pm 1$ Hz. The natural abundance of ^{13}C is 1.1%, but six carbon nuclei are bonded to molybdenum; therefore, approximately 6.6% of the $\text{Mo}(\text{CO})_6$ molecules will have a ^{13}C adjacent to molybdenum. From a solution ^{13}C NMR study of $[\text{M}(\text{CO})_6]$ complexes, Mann reported $^1J(^{95}\text{Mo},^{13}\text{C}) = 68$ Hz.²⁰ Moreover, it is also apparent from the inset shown in Figure 3

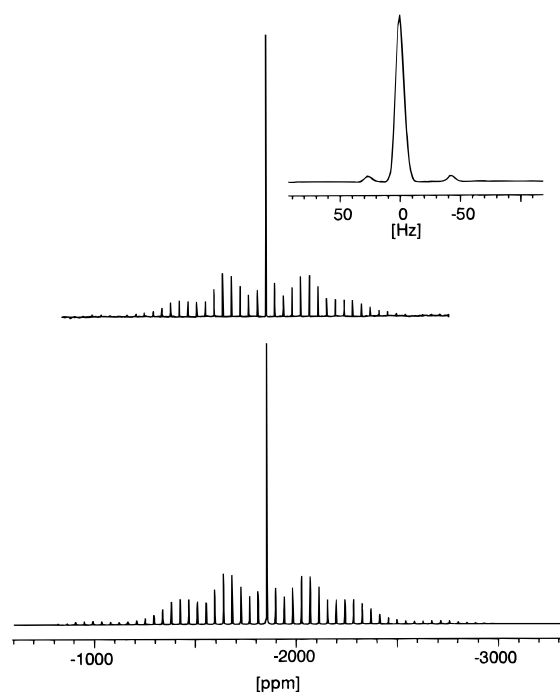


Figure 3. ^{95}Mo MAS NMR spectra of a powder sample of $\text{Mo}(\text{CO})_6$ obtained at 9.4 T with a spinning rate of 1122 Hz. The experimental spectrum is shown on the top trace; 572 scans, 10 s recycle delay. The theoretical spectrum shown on the lower trace was calculated using the values given in Table 1. The inset shows an expansion of the central transition, indicating the presence of ^{13}C satellites.

that there is a significant $^{13}\text{C}/^{12}\text{C}$ isotope effect on the molybdenum chemical shielding, $^1\Delta\sigma_{\text{Mo}}(^{13}/^{12}\text{C}) \approx \sigma_{\text{Mo}}(^{12}\text{C}) - \sigma_{\text{Mo}}(^{13}\text{C}) = -0.316$ ppm. To the best of our knowledge, this is the first experimental measurement of $^1\Delta\sigma_{\text{Mo}}(^{13}/^{12}\text{C})$. The isotope shift observed here is comparable to the $^{18}/^{16}\text{O}$ isotope effect observed for Mo shielding of the molybdate ion, $^1\Delta\sigma_{\text{Mo}}(^{18}/^{16}\text{O}) = -0.25 \pm 0.01$ ppm.²¹ For complexes of the type $\text{M}(\text{XY})_6$, Jameson and co-workers have shown how the isotope shift can be related to the derivative of the chemical shielding (nucleus M) with respect to bond length.²² Details concerning the evaluation of this derivative will be given elsewhere. It should be noted that the temperature dependence of $\sigma(^{95}\text{Mo})$ for $\text{Mo}(\text{CO})_6$ is related to the same derivative, $[\partial\sigma(^{95}\text{Mo})/\partial r]_e$. The magnitude of the isotope shift observed here and the significant temperature dependence of $\sigma(^{95}\text{Mo})$ for $\text{Mo}(\text{CO})_6$,²³ -0.29 ppm deg^{-1} , are reasonable given that the known range of ^{95}Mo chemical shifts exceeds 5000 ppm.

Here we briefly discuss what is known about the crystal structure of $\text{Mo}(\text{CO})_6$ and the relationship between the structure and the NMR parameters obtained in this study. Early single-crystal X-ray diffraction studies of $\text{Cr}(\text{CO})_6$, $\text{Mo}(\text{CO})_6$, and $\text{W}(\text{CO})_6$ indicated that the crystals of these compounds were orthorhombic.²⁴ The crystal structure of $\text{Cr}(\text{CO})_6$ has been investigated more recently by X-ray and neutron diffraction.^{25–27} The space group is $Pnma$, $Z = 4$. The structure indicates the presence of a symmetry plane which contains the chromium and two carbonyl groups which are trans to one another. Single-crystal infrared and Raman studies of $\text{Cr}(\text{CO})_6$, $\text{Mo}(\text{CO})_6$, and $\text{W}(\text{CO})_6$ also support the contention that the crystal space groups of these three compounds are the same.²⁸ The presence of a reflection plane requires that one component of the CS and EFG tensors must lie perpendicular to that plane. The results of the present NMR study indicate that δ_{33} and q_{22} must be perpendicular to the reflection plane. As a point of interest, the ^{95}Mo NMR spectrum was analyzed before we had any knowledge of the crystal structure. Although the crystal structure of the group

6 hexacarbonyls implies that four peaks (relative intensity 2:2:1:1) should be observed in the ^{13}C and ^{17}O MAS NMR spectra of $\text{Cr}(\text{CO})_6$, $\text{Mo}(\text{CO})_6$, and $\text{W}(\text{CO})_6$, only one isotropic peak was observed.²⁹ It is quite likely that the distortion from octahedral symmetry is rather small. Indeed, in the case of $\text{Cr}(\text{CO})_6$, the Cr–C bond lengths are very similar (1.9132, 1.9105, 1.9125, and 1.9185 Å); also, the C–Cr–C bond angles ($90.0 \pm 0.9^\circ$ and $180.0 \pm 0.6^\circ$) are very close to those required for perfect octahedral symmetry.

Carbon-13, ^{17}O , ^{95}Mo , and ^{97}Mo spin–lattice relaxation times for $\text{Mo}(\text{CO})_6$ dissolved in chloroform solution have been measured by Brownlee and co-workers.^{30,31} From the ratio $T_1(^{95}\text{Mo})/T_1(^{97}\text{Mo})$, the authors were able to establish that the quadrupolar mechanism is the only important mechanism for both isotopes. Using a rotation correlation time derived from the ^{13}C relaxation data, the authors calculated an effective ^{95}Mo quadrupolar coupling constant of 133 ± 15 kHz. It was argued that the close agreement between the value determined in chloroform solution and in the early solid-state experiment¹⁸ indicates that the geometry of the complex in solution is similar to that in the solid state. That is, it was postulated that there is a permanent static EFG which arises from small deviations from perfect octahedral symmetry. While the EFG at molybdenum in the solid state must arise from such distortions, it is not clear why the geometry of $\text{Mo}(\text{CO})_6$ in solution should result in a permanent static EFG at Mo. We are unaware of any theoretical reason for the symmetry at Mo being different than O_h . Also, recent theoretical calculations are consistent with the octahedral geometry for $\text{Mo}(\text{CO})_6$.³² As well, electron diffraction data provide no evidence for a distorted octahedron in the gas phase.³³ Relaxation data in other solvents and at more than one temperature and applied magnetic field might help clarify the situation.

Finally, we mention that solid $\text{Mo}(\text{CO})_6$ is an excellent setup sample for solid-state ^{95}Mo MAS NMR studies. At 9.4 T, the free-induction decay can easily be observed with one scan, and the narrow line width makes it a sensitive probe for setting the magic angle accurately. Furthermore, with the NMR parameters presented here, one can easily calculate the spectral appearance at any field.

$\text{Mo}(\text{CO})_5(\text{MeDBP})$ and $\text{Mo}(\text{CO})_5(\eta^1\text{-dppm})$. In a recent ^{31}P NMR study of solid $\text{Mo}(\text{CO})_5(\text{MeDBP})$, we noticed several weak peaks within a frequency range of ± 500 Hz of an intense isotropic peak in ^{31}P NMR spectra acquired with rapid MAS.³⁴ These satellite peaks arise from spin–spin coupling of the ^{31}P with ^{95}Mo and ^{97}Mo . It is well known that heteronuclear direct-dipolar interactions involving quadrupolar nuclei are not completely eliminated by MAS because the quadrupolar nuclei are not completely quantized along the applied magnetic field direction.³⁵ Thus, the detailed line shape of the satellite peaks depends on the effective dipolar coupling constants, $R(^{95}\text{Mo}, ^{31}\text{P})$ and $R(^{97}\text{Mo}, ^{31}\text{P})$, the indirect spin–spin coupling constants, $^1J(^{95}\text{Mo}, ^{31}\text{P})$ and $^1J(^{97}\text{Mo}, ^{31}\text{P})$, the $^{95/97}\text{Mo}$ nuclear quadrupole coupling constants, and other parameters. In order to fully analyze the ^{31}P MAS spectra, it is desirable to have as much information as possible about the electric-field gradient at molybdenum (*e.g.*, $\chi(^{95}\text{Mo})$, η , and the orientation of the EFG tensor relative to the molybdenum–phosphorus bond axis, *etc.*). In the case of solid $\text{Mo}(\text{CO})_5(\text{MeDBP})$, such data were not available in the literature; in fact, it was this lack of information about the ^{95}Mo quadrupolar tensors that prompted the current investigation. Very few $^{95/97}\text{Mo}$ quadrupolar coupling constants appear to be available for organomolybdenum compounds. We are aware of one nuclear quadrupole resonance (NQR) investigation of two compounds, $\text{Mo}(\text{CO})_5\text{PPh}_3$ and *cis*- $\text{Mo}(\text{CO})_4$ -

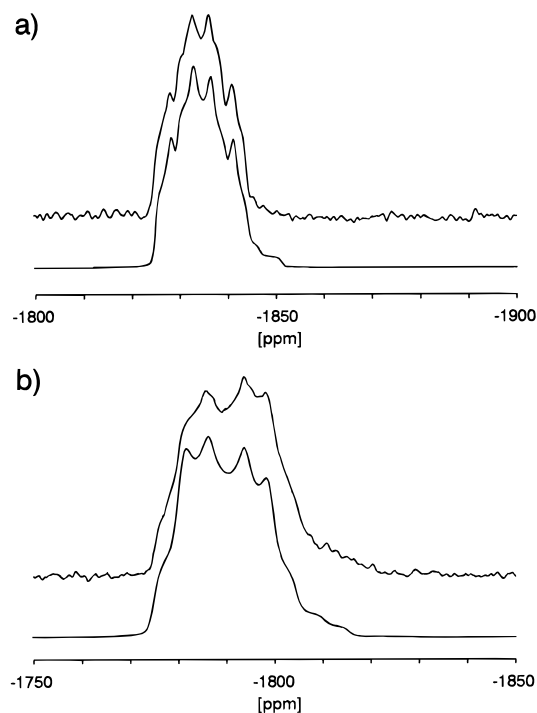


Figure 4. ^{95}Mo MAS NMR spectra of powder samples of $\text{Mo}(\text{CO})_5$ - (MeDBP) (a) and $\text{Mo}(\text{CO})_5(\eta^1\text{-dppm})$ (b) obtained at 9.4 T. The experimental spectra are shown on the top traces, and the theoretical spectra on the lower traces have been calculated using the values given in Table 1; (a) 19253 scans, 4 s recycle delay, spinning rate 2.6 kHz and (b) 30291 scans, 5 s recycle delay, spinning rate 2.6 kHz.

$(\text{PPh}_3)_2$ (see Table 1).³⁶ The ^{95}Mo nuclear quadrupolar coupling constant for mesitylene molybdenum tricarbonyl has been deduced from NMR relaxation measurements in solution and from NMR measurements of dielectrically aligned molecules.³⁷ The latter experiment indicates $\chi = 0.945 \pm 0.050$ MHz, with the largest component of the EFG tensor being along the dipole moment of the complex (the C_3 axis). As required by symmetry, the asymmetry parameter, η , is zero. From ^{95}Mo , ^{17}O , and ^{13}C NMR relaxation data in chloroform or methylene chloride solutions, Brownlee and co-workers³⁸ concluded that $\chi(^{95}\text{Mo}) = 1.2 \pm 0.2$ MHz for compounds belonging to the class $[\text{Mo}(\text{CO})_3(\eta^6\text{-C}_6\text{H}_6\text{-}n\text{Me}_n)]$.

The ^{95}Mo MAS NMR spectrum of solid $\text{Mo}(\text{CO})_5(\text{MeDBP})$ is shown in Figure 4, together with the calculated spectrum. The ^{95}Mo NMR line shape depends on $\chi(^{95}\text{Mo})$, η , and $^1J(^{95}\text{Mo}, ^{31}\text{P})$; the best-fit parameters are shown in Table 1. X-ray diffraction data indicate that the eight molecules in the monoclinic unit cell are crystallographically equivalent. The value of χ , 1.03 MHz, is somewhat smaller than the value obtained by NQR for a related compound, $\text{Mo}(\text{CO})_5\text{PPh}_3$, 1.972 MHz; however, the NQR data were obtained at 77 K.³⁶ Values of χ invariably increase with decreasing temperature; furthermore, there is no reason for the electric-field gradients in these two phosphine complexes to be the same. Interestingly, the ^{31}P MAS NMR spectrum of solid $\text{Mo}(\text{CO})_5(\text{MeDBP})$ indicates that the sign of the ^{95}Mo nuclear quadrupolar coupling constant must be negative. Therefore, it is reasonable to conclude that $\chi(^{95}\text{Mo})$ will be negative for all compounds of this type, $\text{Mo}(\text{CO})_5\text{PR}_3$. Also, analysis of the ^{31}P MAS NMR spectrum confirms that $^1J(^{95}\text{Mo}, ^{31}\text{P}) = 130 \pm 10$ Hz, in excellent agreement with the value determined in solution.¹¹ As in the case of $\text{Na}_2\text{MoO}_4 \cdot 2\text{H}_2\text{O}$, the experimental spectrum was simulated using convolution with a Gaussian peak 27 Hz wide.

The asymmetry parameter of the ^{95}Mo EFG tensor for $\text{Mo}(\text{CO})_5(\text{MeDBP})$ is clearly not 0. For approximately octahedral

complexes of the type $M(\text{CO})_5\text{PR}_3$, where M is some metal, it might be tempting to assume η is 0; however, this is not required by symmetry. Certainly, the triphenylphosphine ligand is more symmetrical than the 5-methyl-dibenzophosphole ligand; this is reflected in a smaller value of η for $\text{Mo}(\text{CO})_5\text{PPh}_3$, 0.064 ± 0.008 . Although the asymmetry parameter is non-zero, the largest component of the EFG tensor is probably close to the Mo–P bond vector; this approximate orientation is required to yield the residual dipolar splittings observed in the ^{31}P CP/MAS spectra of $\text{Mo}(\text{OC})_5(\text{MeDBP})$.³⁴ Clearly, a single-crystal NMR study would be required in order to establish the orientation of the EFG tensor.

Solid-state ^{95}Mo MAS NMR spectra were also obtained for $\text{Mo}(\text{CO})_5(\eta^1\text{-dppm})$ (Figure 4). Best-fit parameters are given in Table 1. The ^{31}P CP/MAS spectrum of this compound shows clear satellites due to coupling with $^{95/97}\text{Mo}$; however, the analysis is more complicated in this case because of the presence of an additional $^1J(^{31}\text{P}, ^{31}\text{P})$ coupling constant, which is of similar magnitude, 145 Hz. The ^{95}Mo chemical shift observed in the solid state is similar to that observed in solution.³⁹

Conclusions

From the results presented here, it is clear that solid-state MAS ^{95}Mo NMR studies of organometallic complexes of molybdenum are feasible, particularly if the compounds are known to give relatively narrow ^{95}Mo NMR peaks in solution. Because the second-order quadrupolar line broadening depends on the inverse of the applied magnetic field, these studies will be facilitated by working at the highest possible fields. In order to eliminate anisotropic shielding at high applied field strengths, it will be necessary to spin the samples rapidly. The major issue in observing ^{95}Mo in the solid state is sensitivity. In selecting the best pulse sequence, one will need to compromise either line shape and base line, by using single-pulse experiments, or intensity, by using echo sequences.

Finally, this study clearly demonstrates that one can uncover considerable information concerning molybdenum shielding and EFG tensors. With recent encouraging developments in the computation of transition metal shielding tensors⁴⁰ it will become increasingly desirable to have such information.

Acknowledgment. We thank the Natural Sciences and Engineering Research Council of Canada (NSERC) for financial assistance in the form of equipment and operating grants (R.E.W.). J.H.N. thanks the donors of the Petroleum Research Fund, administered by the American Chemical Society, for financial support. All solid-state spectra were recorded at the Atlantic Region Magnetic Resonance Centre, which is also supported by NSERC. We thank Gabriel C. Ossenkamp for preparing $\text{Mo}(\text{CO})_5(\eta^1\text{-dppm})$ and Professor C. J. Jameson for discussions concerning isotope shifts. R.E.W. acknowledges the Canada Council for a Killam Research Fellowship.

References and Notes

- (1) Granger, P. In *Encyclopedia of Nuclear Magnetic Resonance*; Grant, D. M., Harris, R. K., Eds.; John Wiley & Sons: Chichester, U.K., 1996; Vol. 6, pp 3889–3900.
- (2) Malito, J. *Ann. Rep. NMR Spectrosc.* **1997**, 33, 151.

- (3) Minelli, M.; Enemark, J. H.; Brownlee, R. T. C.; O'Connor, M. J.; Wedd, A. G. *Coord. Chem. Rev.* **1985**, 68, 169.
- (4) Rehder, D. In *Multinuclear NMR*; Mason, J., Ed.; Plenum Press: New York, 1987; p 479.
- (5) Pregosin, P. S. In *Transition Metal Nuclear Magnetic Resonance*; Pregosin, P. S., Ed.; Elsevier: Amsterdam, 1991; pp 67–81.
- (6) Freude, D.; Haase, J. In *NMR, Basic Principles and Progress*; Diehl, P., Fluck, E., Günther, H., Kosfeld, R., Seelig, J., Eds.; Springer-Verlag: Berlin, 1993; Vol. 29, pp 1–90.
- (7) Stauss, G. H. *J. Chem. Phys.* **1964**, 40, 1988.
- (8) Amoureux, J. P.; Fernandez, C.; Granger, P. In *Multinuclear Magnetic Resonance in Liquids and Solids - Chemical Applications*; Granger, P., Harris, R. K., Eds.; Kluwer Academic Publishers: Dordrecht, The Netherlands, 1990; pp 409–424.
- (9) Taulelle, F. In *Multinuclear Magnetic Resonance in Liquids and Solids - Chemical Applications*; Granger, P., Harris, R. K., Eds.; Kluwer Academic Publishers: Dordrecht, The Netherlands, 1990; pp 393–407.
- (10) Man, P. P. In *Encyclopedia of Nuclear Magnetic Resonance*; Grant, D. M., Harris, R. K., Eds.; John Wiley & Sons: Chichester, U.K., 1996; Vol. 6, pp 3838–3848.
- (11) Maitra, K.; Wilson, W. L.; Jemin, M. M.; Yeung, C.; Rader, W. S.; Redwine, K. D.; Striplin, D. P.; Catalano, V. J.; Nelson, J. H. *Synth. React. Inorg. Met.-Org. Chem.* **1996**, 26, 967.
- (12) (a) Koelle, U. *J. Organomet. Chem.* **1977**, 133, 53. (b) Hor, T. S. *A. J. Organomet. Chem.* **1987**, 319, 213.
- (13) Kautt, W. D.; Krüger, H.; Lutz, O.; Maier, H.; Nolle, A. *Z. Naturforsch.* **1976**, 31A, 351.
- (14) Matsumoto, K.; Kobayashi, A.; Sasaki, Y. *Bull. Chem. Soc. Jpn.* **1975**, 48, 1009.
- (15) Edwards, J. C.; Adams, R. D.; Ellis, P. D. *J. Am. Chem. Soc.* **1990**, 112, 8349.
- (16) Lynch, G. F.; Segel, S. L. *Can. J. Phys.* **1972**, 50, 567.
- (17) Mastikhin, V. M.; Lapina, O. B.; Maximovskaya, R. I. *Chem. Phys. Lett.* **1988**, 148, 413.
- (18) Nolle, A. *Z. Phys.* **1977**, A280, 231.
- (19) Shirley, W. M. *Z. Phys. Chem.* **1987**, 152, 41.
- (20) Mann, B. E. *J. Chem. Soc., Dalton Trans.* **1973**, 2012.
- (21) Buckler, K. U.; Haase, A. R.; Lutz, O.; Müller, M.; Nolle, A. *Z. Naturforsch.* **1977**, 32A, 126. Lutz, O.; Nolle, A.; Kroneck, P. *Z. Phys.* **1977**, A282, 157.
- (22) Jameson, C. J.; Rehder, D.; Hoch, M. *J. Am. Chem. Soc.* **1987**, 109, 2589.
- (23) Andrews, G. T.; Colquhoun, I. J.; McFarlane, W.; Grim, S. O. *J. Chem. Soc., Dalton Trans.* **1982**, 2353.
- (24) Rüdorff, W.; Hofmann, U. *Z. Phys. Chem.* **1935**, B28, 351.
- (25) Whitaker, A.; Jeffery, J. W. *Acta Crystallogr.* **1967**, 23, 977 and 984.
- (26) Jost, A.; Rees, B.; Yelon, W. B. *Acta Crystallogr.* **1975**, B31, 2649.
- (27) Rees, B.; Mitschler, A. *J. Am. Chem. Soc.* **1976**, 98, 7918.
- (28) Adams, D. M.; Taylor, I. D. *J. Chem. Soc., Faraday Trans. 2* **1982**, 78, 1051.
- (29) Oldfield, E.; Keniry, M. A.; Shinoda, S.; Schramm, S.; Brown, T. L.; Gutowsky, H. S. *J. Chem. Soc., Chem. Commun.* **1985**, 791.
- (30) Brownlee, R. T. C.; O'Connor, M. J.; Shehan, B. P.; Wedd, A. G. *J. Magn. Reson.* **1985**, 61, 22.
- (31) Brownlee, R. T. C.; Shehan, B. P. *J. Magn. Reson.* **1986**, 66, 503.
- (32) Ehlers, A. W.; Frenking, G. *J. Am. Chem. Soc.* **1994**, 116, 1514.
- (33) Arnesen, S. P.; Seip, H. M. *Acta Chem. Scand.* **1966**, 20, 2711.
- (34) Eichele, K.; Wasylishen, R. E.; Maitra, K.; Nelson, J. H.; Britten, J. F. *Inorg. Chem.*, in press.
- (35) Harris, R. K.; Olivieri, A. C. *Prog. NMR Spectrosc.* **1992**, 24, 435.
- (36) Blumer, D. J.; Cheng, C. P.; Brown, T. L. *Chem. Phys. Lett.* **1977**, 51, 473.
- (37) Huis, L.; Pouwels, P. J. W.; MacLean, C. *Mol. Phys.* **1990**, 70, 879.
- (38) Brownlee, R. T. C.; O'Connor, M. J.; Shehan, B. P.; Wedd, A. G. *Aust. J. Chem.* **1986**, 39, 931.
- (39) Alyea, E. C.; Ferguson, G.; Fisher, K. J.; Gossage, R. A.; Jennings, M. C. *Polyhedron* **1990**, 9, 2393.
- (40) (a) Jameson, C. J. In *Nuclear Magnetic Resonance—A Specialist Periodical Report*; Webb, G. A., Ed.; Royal Society of Chemistry: Cambridge, Great Britain, 1996; Vol. 25 and previous volumes in this series. (b) Bühl, M. *Chem. Phys. Lett.* **1997**, 267, 251. (c) Nakatsuji, H.; Sugimoto, M. *Inorg. Chem.* **1990**, 29, 1221. (d) Nakatsuji, H.; Sugimoto, M.; Saito, S. *Inorg. Chem.* **1990**, 29, 3095. (e) Combariza, J. E.; Barfield, M.; Enemark, J. H. *J. Phys. Chem.* **1991**, 95, 5463. (f) Teruel, H.; Sierralta, A. *Polyhedron* **1996**, 15, 2215.